Protein Rearrangements Underlying Slow Inactivation of the *Shaker* K^+ Channel

E. Loots and E.Y. Isacoff

From the Department of Molecular & Cell Biology, University of California, Berkeley, Berkeley, California 94720-3200

ABSTRACT Voltage-dependent ion channels transduce changes in the membrane electric field into protein rearrangements that gate their transmembrane ion permeation pathways. While certain molecular elements of the voltage sensor and gates have been identified, little is known about either the nature of their conformational rearrangements or about how the voltage sensor is coupled to the gates. We used voltage clamp fluorometry to examine the voltage sensor (S4) and pore region (P-region) protein motions that underlie the slow inactivation of the *Shaker* K^+ channel. Fluorescent probes in both the P-region and S4 changed emission intensity in parallel with the onset and recovery of slow inactivation, indicative of local protein rearrangements in this gating process. Two sequential rearrangements were observed, with channels first entering the P-type, and then the C-type inactivated state. These forms of inactivation appear to be mediated by a single gate, with P-type inactivation closing the gate and C-type inactivation stabilizing the gate's closed conformation. Such a stabilization was due, at least in part, to a slow rearrangement around S4 that stabilizes S4 in its activated transmembrane position. The fluorescence reports of S4 and P-region fluorophore are consistent with an increased interaction of the voltage sensor and inactivation gate upon gate closure, offering insight into how the voltage-sensing apparatus is coupled to a channel gate.

KEY WORDS: inactivation • fluorescence • K^+ channel • pore • S4

INTRODUCTION

Upon membrane depolarization, many voltage-gated ion channels open and inactivate, producing a transient ionic current. Channels must first recover from inactivation before they may again conduct ions in response to subsequent depolarization, providing the cell with a gauge of the magnitude, duration, and frequency of excitatory activity.

Inactivation of K^+ channels occurs via several distinct mechanisms. Fast inactivation is due to block of the internal mouth of the open channel by the channel's NH_2 terminus, and has therefore been called N-type inactivation (Timpe et al., 1988; Hoshi et al., 1990, Zagotta et al., 1990; Isacoff et al., 1991). Slow inactivation is composed of multiple components and is influenced by mutations in the pore region (P-region)[1] and S6 (Timpe et al., 1988; Iverson and Rudy, 1990; Hoshi et al., 1991; Lopez-Barneo et al., 1993; Yang et al., 1997; Olcese et al., 1997). Since this protein segment is encoded by the COOH-terminal exon of the *Shaker* K^+ channel, slow inactivation was originally called C-type inactivation. Recently, an apparently distinct form of slow inactivation was identified and called P-type inactivation (De Biasi et al., 1993; Yang et al., 1997). P- and C-type inactivation, both forms of slow inactivation that block current flow, have previously been distinguished by the fact that C-type alters the voltage dependence of gating charge movement (Olcese et al., 1997), while P-type inactivated channels do not display such a change in voltage sensitivity. This has cast uncertainty on whether earlier studies, which did not measure the voltage dependence of charge movement (but often called slow inactivation C-type inactivation), were looking at what the recent studies characterize as P- and C-type inactivation.

Slow inactivation of the channel appears to involve a reorientation of the residues in the P-region (Boland et al., 1994; Liu et al., 1996; Cha and Bezanilla, 1997). Since the P-region forms the outer mouth of the pore (for references see Gross and MacKinnon, 1996; Naranjo and Miller, 1996), as well as the narrowest part of the pore where K^+ ions bind and ion selectivity is conferred (Yool and Schwarz, 1991; Heginbotham et al., 1994; Lu and Miller, 1995; Kurz et al., 1995; Pascual et al., 1995; Harris et al., 1997), this movement has been proposed to stop ion conduction by squeezing the pore shut in the P-region (Yellen et al., 1994; Liu et al., 1996), thus closing off access between the deep pore and the extracellular solution (Harris et al., 1998). This closure may

Address correspondence to E.Y. Isacoff, Department of Molecular & Cell Biology, University of California, Berkeley, 271 Life Science Addition, Berkeley, CA 94720-3200. Fax: 510-643-6791; E-mail: chud@uclink.berkeley.edu

[1] *Abbreviations used in this paper:* F-V, fluorescence–voltage; G-V, conductance–voltage; P-region, pore region; TMRM, tetramethylrhodamine maleimide.

J. Gen. Physiol. © The Rockefeller University Press • 0022-1295/98/10/377/13 $2.00
Volume 112 October 1998 377–389
http://www.jgp.org

occur near a K^+-selective binding site, since slow inactivation appears to require the prior evacuation of a K^+ ion from the pore (Baukrowitz and Yellen, 1996). It is not known whether this inactivation rearrangement is limited to a small motion at the COOH-terminal end of the P-region. Nor is it understood how this motion is related to a recent recasting of slow inactivation into two processes that have been called P- and C-type inactivation (Olcese et al., 1997; Yang et al., 1997).

One of the obstacles to elucidating the mechanism of slow inactivation using traditional voltage clamp measurements has been that transitions between closed states in the activation pathway and inactivated states, and between one inactivated state and another, can be difficult to tease apart because all of these states are nonconducting and transitions between them generate little or no detectable current. We circumvented this problem by using voltage clamp fluorimetry on channels to which a fluorophore has been attached site specifically (Mannuzzu et al., 1996; Cha and Bezanilla, 1997). In this way, we were able to monitor structural rearrangements of the channel protein that change the environment, and thus the emission, of the fluorophore, whether or not the rearrangements produce a measurable change in current.

We find that the emission of a fluorophore attached either to the NH_2-terminal end of the P-region or to that of S4 changes in parallel with the onset and recovery of slow inactivation, suggesting that a rearrangement around these domains underlies inactivation gating. The results are consistent with two sequential rearrangements around the P-region and S4 during the onset of inactivation. The first rearrangement shuts the channel and makes it behave as if it carries the W434F mutation. The second rearrangement shifts the voltage dependence of gating charge movement and yields a stabilized closed conformation. We refer to these successive steps as P- and C-type inactivation, respectively, in keeping with recent work that used those names to refer to the W434F mutation and to the shift in the voltage dependence of charge movement (Olcese et al., 1997; Yang et al., 1997). Our interpretation is that both forms of inactivation involve a single external gate. We propose that this gate is first closed in P-type inactivation and that a further rearrangement in or around S4 stabilizes this closed conformation, in part by stabilizing S4 in its activated transmembrane position.

MATERIALS AND METHODS

Molecular Biology

Site-directed mutagenesis was done by the dut- ung- method (Kunkel, 1985) and examined by S^{35} sequencing. Unless otherwise denoted, the standard composition of the channel was *Shaker* H4 (Δ6-46/W434/C245V/C462A). Positions 245 and 462 were changed from cysteines originally to avoid their possible labeling by tetramethylrhodamine maleimide (TMRM), but this later proved to be unnecessary.

cRNA was transcribed using T7 Ambion mMessage mMachine. Injection of the oocytes (50 nl mRNA, at 1 ng/nl), native cysteine blocking with tetraglycine maleimide, and attachment of the fluorescent probe TMRM were as previously described (Mannuzzu et al., 1996). In brief, 3-4 d after injection and incubation at 12°C, oocytes were incubated for 1 h in tetraglycine maleimide to block native cysteines at room temperature. After 14 h of incubation at room temperature, oocytes were washed and labeled with 50 μM TMRM in a high potassium solution containing (mM) 92 KCl, 0.75 $CaCl_2$, 1 $MgCl_2$, 10 HEPES, pH 7.5, 30 min on ice, and kept in this solution (in the dark, at 12°C) until voltage clamped at room temperature. Coinjections were performed on indicated dilutions of cRNAs that gave bands of equal intensity when run side by side on the same gel. Linked tetramers were made in JC12123 cells, with the linker of 10 glutamines that was described previously (Isacoff et al., 1990).

Voltage Clamp Fluorimetry and Analysis

Two-electrode voltage clamp fluorimetry was performed as described previously (Mannuzzu et al., 1996), using a Dagan CA-1 amplifier (Dagan Corp., Minneapolis, MN), illuminated with a 100-W mercury arc lamp, on an IM35 microscope (Carl Zeiss, Inc., Thornwood, NY) using a 10× 0.5 nA fluorescence objective (Nikon Inc., Melville, NY). Photometry was performed with a photomultiplier tube (HC120-05; Hamamatsu Phototonics, Bridgewater, NJ). The voltage clamp, photomultiplier and Uniblitz shutter (Vincent Associates, Rochester, NY) were digitized and controlled by a Digidata-2000 board and PClamp 6 software, respectively (Axon Instruments, Foster City, CA).

The bath solutions consisted of (mM) 110 NaMes, 2 KMes, 2 $CaMes_2$, 10 HEPES, pH7.5 (for pH 5.6 Mes acted as the buffer), or 110 KMes, 2 $CaMes_2$, 10 HEPES, pH 7.5. Oocytes were washed before being placed in the bath and bath solution was constantly perfused through the chamber during recording. The excitation light was reduced by neutral density filters (Carl Zeiss, Inc.) with either a 5% transmission or two neutral density filters in series (25 and 5% transmission) resulting in 1.25% transmission. Light was filtered with an HQ 535/50 excitor, an HQ 610/75 emitter, and a 565LP dichroic (Chroma Technology, Brattleboro, VT). The voltage output of the photomultiplier was low pass filtered at half the sampling frequency with an eight-pole Bessel filter (Frequency Devices Inc., Haverhill, MA). A minimum of a 2-min rest interval at the holding potential of −80 mV was given between pulses. Solutions were exchanged until current–voltage relations indicated no further change in reversal potential (usually 10 min). All measurements on conducting (424C-TMRM/W434) channels were made under continuous perfusion. Data analysis was done with the Clampfit program of PClamp 6 and, in some cases, analyzed further and plotted with Origin (Microcal Software, Inc., Northampton, MA). Fluorescence and current traces were normalized, but not averaged unless so noted. All values are mean ± SEM. Data is included for oocytes with peak ionic currents of 50–120 μA for monomers, and of 15–100 μA for the linked tetramers.

RESULTS

A Fluorescence Change That Correlates with Slow Inactivation

Shaker H4 (Δ6-46/C245V/C462A/S424C) channels (with the NH_2-terminal inactivation ball deleted, cysteines in S2 and S6 mutated to valine and alanine, and a single cysteine added at 424, in the NH_2-terminal end of the

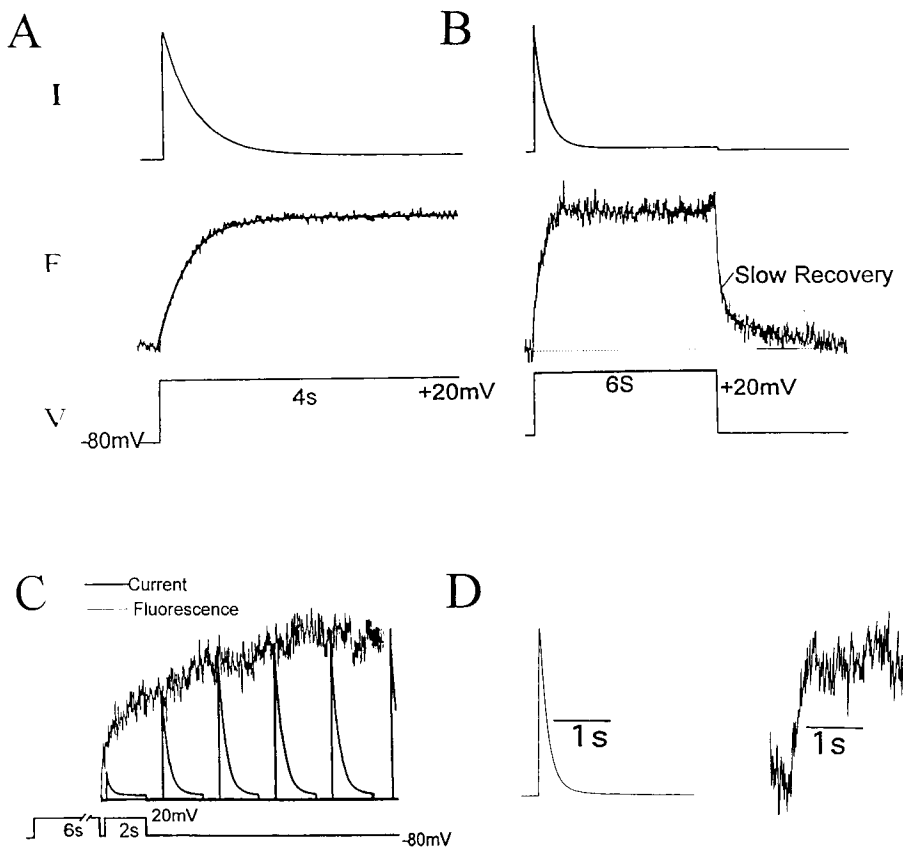

FIGURE 1. Correlation of slow inactivation of ionic current and fluorescence of 424C-TMRM channels. (*A*) Fluorescence (*F*) increases during a voltage step (*V*) with the kinetics of current (*I*) inactivation (solid line superimposed on fluorescence trace is time course of current inactivation from a monoexponential fit). Tau for the fluorescence was 300 ± 22 (n = 7) and the Tau for the current decay was 289 ± 31 (n = 6). (*B*) Upon repolarization, fluorescence recovery consists of fast and slow components. (*C*) The slow component of fluorescence recovery follows the kinetics of recovery of the ionic current. The slow component of fluorescence recovery (*noisy trace*) was taken from *B*, starting at point indicated, and inverted and superimposed on a series of currents evoked by identical test depolarizations (*bottom*) given at varying intervals after a 6-s depolarization (not shown). The Taus for the current recovery and fluorescence decay were 2,344 ± 212 and 2,363 ± 205 ms (n = 3), respectively. (*D*) Fluorescence follows current inactivation in channels predicted to have, at most, only one labelable subunit (1:10 cRNA coinjection ratio of W434/S424C:W434/S424), indicating that the change in fluorescence emission depends on gating-induced changes in TMRM microenvironment, rather than on TMRM–TMRM interaction between subunits. In all cases, depolarization was preceded by 2 min of rest at −80 mV.

P-region) were expressed in *Xenopus* oocytes, and labeled at cysteine 424 with the thiol reagent TMRM (see MATERIALS AND METHODS). Other positions for the incorporation of a labelable cysteine were tried throughout the external loops of the channel, although we concentrated on the pore region considering previous data that suggested it plays a role in slow inactivation. While some sites, such as 255 and 352, demonstrated fluorescence changes, the changes were far too fast to be correlated with inactivation (not shown). However, S424C-TMRM channels showed pronounced slow fluorescence changes.

Prolonged depolarization opened and then slowly inactivated these channels, producing a current with a time constant of decay of 289 ± 31 ms (n = 6) for depolarizations of ≥+20 mV (Fig. 1 *A*). This inactivation is similar to that described earlier (Tau = 352 ms; Boland et al., 1994) for *Shaker* H4 (Δ6-46/C462A), without the additional mutations C245V and S424C, and without conjugation of TMRM to S424C. Simultaneous measure of fluorescence emission from the 6′ isomer of TMRM showed two components of fluorescence increase (F_{onset}): a small (10–15% of total amplitude) fast component, which occurred on the time scale of channel activation, and a large (85–90% of total amplitude) slow component, with a time constant of 300 ± 22 ms (n = 7), which followed the time course of current inactivation (Fig. 1 *A*).

Channels with only one labelable 424C subunit (either encoded by the linked tetramer S424C-S424-S424-S424 [not shown], or made in oocytes coinjected with a S424:S424C cRNA ratio of 10:1) showed fluorescence changes with similar kinetics, but of smaller magnitude, compared with homotetramers of S424C (Fig. 1 *D*), consistent with each individual fluorophore reporting changes in its environment, rather than interaction with fluorophore on other subunits of the same channel.

The inactivated channels reopened their inactivation gates with a time constant of 2.3 ± 0.2 s (n = 3), as demonstrated by the recovery of the peak ionic current during intervals at the negative holding potential (Fig. 1 *C*). The fluorescence recovery exhibited two components (F_{recov}; Fig. 1 *B*), the slower of which represented ~30% of the total amplitude and had a time constant of 2.4 ± 0.2 s (n = 3), paralleling the recovery of the ionic current (Fig. 1 *C*).

The close agreement between the onset and recovery of current inactivation and 424C-TMRM fluorescence suggests that the closure and reopening of the gate responsible for slow inactivation of this channel is associated with a rearrangement about the NH_2-terminal end of the P-region, where the TMRM was attached.

Perturbation of Inactivation Produces Commensurate Changes in Fluorescence of 424C-TMRM

To see how tightly changes in 424C-TMRM fluorescence are associated with the closure of the gate, we examined the effect on fluorescence of three manipulations that alter the rate of current inactivation: high external K^+ concentration (Lopez-Barneo et al., 1993) and reintroduction of the native cysteine to position 462 (Boland et al., 1994), both of which slow the rate of inactivation, and low external pH (Lopez-Barneo et al., 1993), which accelerates it.

In all three cases, the alteration of the rate of current inactivation was paralleled by a change in the slow component of F_{onset}. In 424C-TMRM/W434/C462A channels, raising external K^+ from 2 to 110 mM slowed both current inactivation and the slow component of F_{onset} by ~2.5-fold (Fig. 2 *A*). Reintroduction of the native cysteine to position 462 slowed both inactivation and the slow component of F_{onset} by ~20-fold (Fig. 2 *B*). In this slowly inactivating C462 channel, lowering pH from 7.5 to 5.6 accelerated both inactivation and the slow component of F_{onset} by ~31 ± 11% and 26 ± 15%, respectively (n = 3; Fig. 2 *C*).

Taken together, these correlations between the onset and recovery of current inactivation and 424C-TMRM fluorescence provide strong evidence that a rearrangement around the NH_2-terminal end of the P-region, at the external mouth of the pore, is involved in the closure and reopening of the inactivation gate.

Influence of Ball Inactivation on the Rearrangement Around 424

It has been shown that channels that have first inactivated by the ball-type mechanism are accelerated in their slow inactivation (Hoshi et al., 1991; Baukrowitz and Yellen, 1995). In C462A channels with the NH_2 terminus intact, current inactivation was fast, consistent

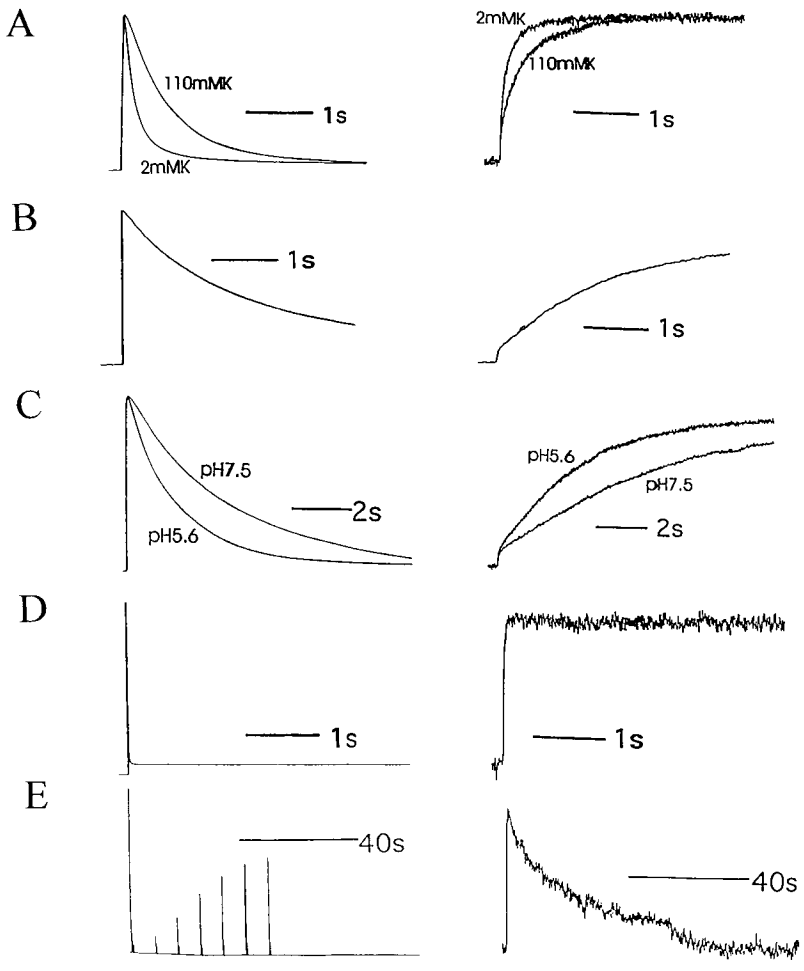

FIGURE 2. 424C-TMRM fluorescence (*right*) follows ionic current inactivation (*left*) under molecular and ionic conditions that alter inactivation rate. (*A*) Exchange of external solution from 2 to 110 mM K^+ slowed both current inactivation and the rate of fluorescence increase of 424C-TMRM/W434/C462A channels ($\tau_{ion\text{-}onset\ (110K)}$ = 742 ± 54 ms, n = 6); $\tau_{fluor\text{-}onset\ (110K)}$ = 689 ± 28 ms, n = 6. (*B*) Channels with a cysteine restored at position 462 (424C-TMRM/W434/C462) were equally slow in current inactivation and fluorescence increase ($\tau_{ion\text{-}onset\ (C462)}$ = 2,476 ± 345 ms; $\tau_{fluor\text{-}onset\ (C462)}$ = 2,412 ± 407 ms, n = 10). (*C*) Exchange of external solution from pH 7.5 to 5.6 accelerated both current inactivation and the rate of fluorescence increase of 424C-TMRM/W434/C462 channels. (*D* and *E*) Restoration of the NH_2-terminal fast inactivation ball to 424C-TMRM/W434/C462A channels accelerated current inactivation and the rate of fluorescence increase (*D*) and slowed current and fluorescence recovery (*E*) compared with control (see Fig. 1). ($\tau_{ion\text{-}onset\ (+ball)}$ = 14 ± 2 ms; $\tau_{fluor\text{-}onset\ (+ball)}$ = 45 ± 3 ms; n = 8.)

with ball block. The depolarization-induced fluorescence increase of 424C-TMRM did not correlate with this inactivation, but it was accelerated by almost sevenfold ($\tau_{ion\text{-}onset\ (ball)} = 14 \pm 2$ ms, $\tau_{fluorophore\text{-}onset\ (ball)} = 45 \pm 3$ ms, $n = 8$; compare Fig. 2, *A* and *D*). This result is consistent with an accelerated closure of the slow inactivation gate, which is masked in the ionic current by the presence of fast ball-type inactivation. Interestingly, the presence of the NH_2-terminal ball dramatically slowed the recovery from slow inactivation of both the ionic current and the fluorescence (compare Figs. 1 *C* and 2 *E*). Since this recovery is slower than the rate of unbinding of the ball from the internal mouth of the channel after repolarization (Hoshi et al., 1990; Zagotta et al., 1990), the result suggests that ball block of the internal mouth of the pore not only accelerates closure of the slow inactivation gate, but also favors entry into a stabilized form of this closed state. This idea is explored further below.

Voltage Dependence of 424C-TMRM Fluorescence

Slow inactivation has been proposed to occur from both closed and open states of the channel (Marom et al., 1994; Olcese et al., 1997). Our measurements support this idea in that the dependence of inactivation on the voltage of 4-s-long prepulses (Inact-V) was located to the left of the conductance–voltage (G-V) relation (Fig. 3 *A*). The Inact-V relation was also steeper than the G-V relation. The fluorescence–voltage (F-V) relation correlated closely with the Inact-V relation, providing further evidence that the rearrangement around position 424 is associated with closure of the slow inactivation gate, and suggesting that this gate can close from intermediate activated states in which the activation gate is closed. As shown earlier for slow inactivation (Hoshi et al., 1991; Levy and Deutsch, 1996), the rate of 424C-TMRM F_{onset} and F_{recov} were voltage dependent over the voltage range of channel activation (Fig. 3 *B*), but F_{onset} was voltage independent at extremes of depolarization. This behavior is consistent with a lack of intrinsic voltage dependence for the closure of the slow inactivation gate.

The Balance Between the Fast and Slow Components of the 424C-TMRM Fluorescence Change

As mentioned above, both the onset and recovery of the fluorescence change of 424C-TMRM had fast and slow components. After 3 min of rest at −80 mV, F_{onset} was mainly slow, with a small fast component (Fig. 4 *A*) that became progressively smaller with longer rest intervals. This balance between relative contributions of the two components changed when channels were preinactivated. The fast component of F_{onset} was larger when a second depolarization occurred before most of the channels had recovered from the inactivation (Fig. 4 *A*). As current recovered from inactivation with longer intervals, the fractional contribution of the slow component to total amplitude increased until return-

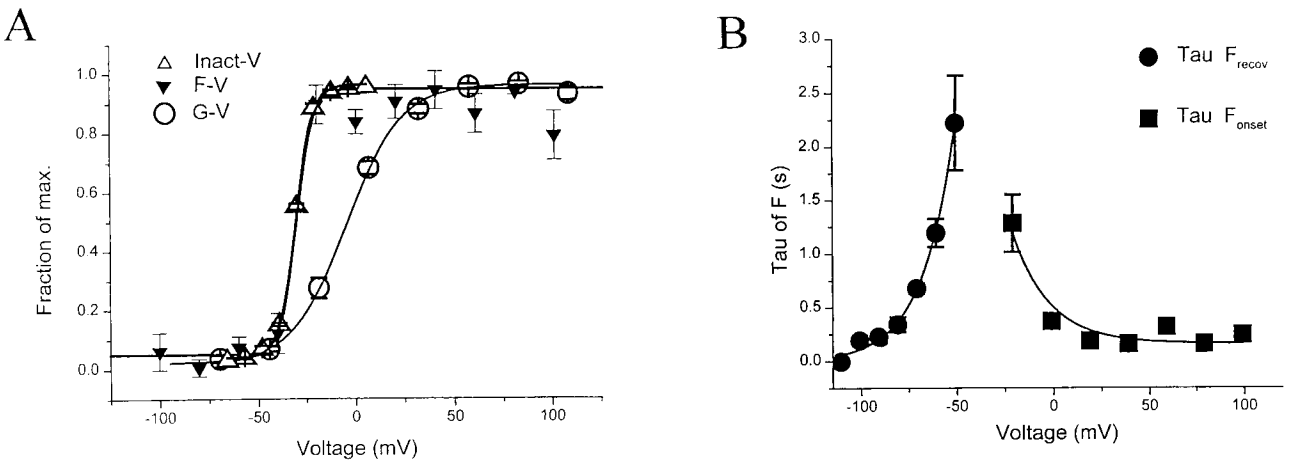

FIGURE 3. Voltage dependence of current inactivation and 424C-TMRM fluorescence. (*A*) Voltage dependencies of channel opening (*G-V*), fluorescence (*F-V*), and current inactivation (*Inact-V*). The F–V relations were obtained from measurements of fluorescence 4 s after the start of a step to the indicated test potential (long enough for the fluorescence change to reach steady state at all test potentials). Inact-V relations were obtained from a measure of the fraction of the maximal decline in current evoked by a step to +20 mV, following a 4-s prepulse to the indicated test potential. The G-V was calculated from steady state, leak-subtracted currents assuming $E_k = -100$ mV. Measurements made in W434/424C-TMRM channels ($n = 10$). Fits are to single Boltzmann functions. (*B*) Voltage dependence of the time constants for F_{onset} (measured from 4-s depolarizations) and F_{recov} (measured from 20-s long tails to indicated potentials, after a 4-s depolarization to 0 mV). Rate of F_{onset} appears to be intrinsically voltage independent since it does not change over a wide range of positive potentials. Fits are to single exponentials.

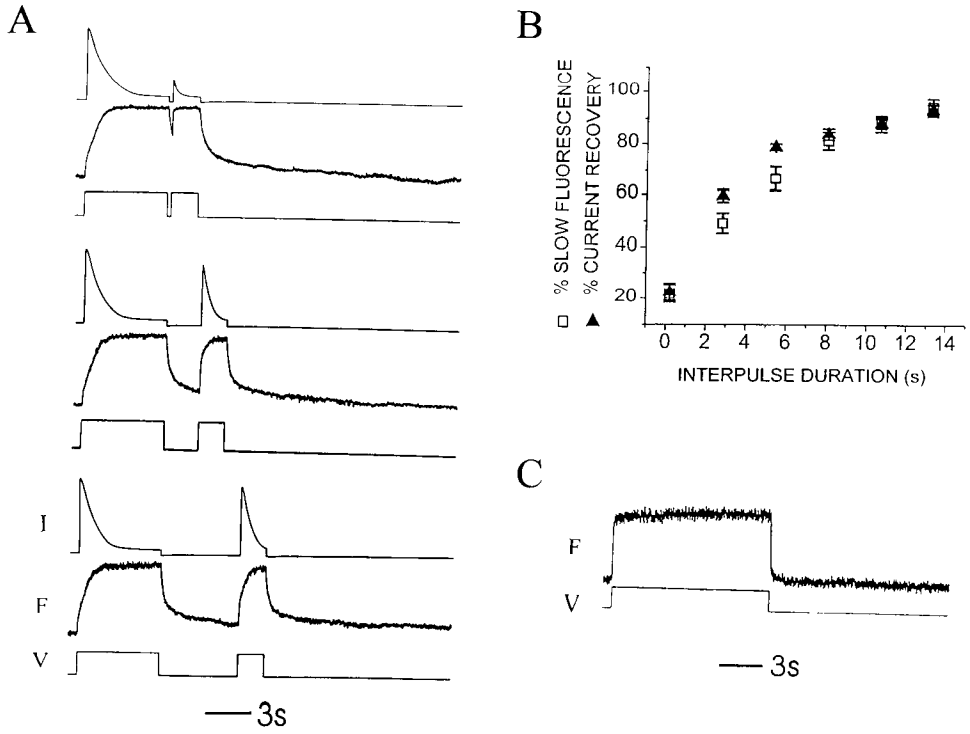

FIGURE 4. P-type inactivation switches kinetics of 424C-TMRM F_{onset} from slow to fast. (*A*) After 3 min at negative voltage (V_{hold} = −80 mV), F_{onset} during a 6-s step to +20 mV of 424C-TMRM/W434/C462A channels is composed of a small fast component and a large slow component. A second depolarization to +20 mV, after a variable interval at −80 mV, evokes an F_{onset} with a larger fractional contribution of the fast component. The relative amplitude of slow component increases with increasing recovery interval. Note that F_{recov} also has fast and slow components. Current (*top*), fluorescence (*middle*), and voltage (*bottom*) for three different intervals in the twin pulse experiment. (*B*) Recovery from inactivation of the ionic current has a similar dependence on interpulse interval, as does the recovery of the slow component of F_{onset}. The observations are consistent with the distribution of channels into two states: noninactivated (slow F_{onset}) and inactivated (fast F_{onset}), with the majority of channels being noninactivated after a long rest at −80 mV. Relative contribution of the two components of F_{onset} was determined from two exponential fits to the fluorescence increase. Current recovery was calculated as $I_{peak\ (step\ 2)}/I_{peak\ (step\ 1)}$. V_{hold} = −80 mV, V_{step} = +20 mV, rest between sets of twin pulses = 3 min. (*C*) Depolarization (to +20 mV) of 424C-TMRM/W434F channels, after 3 min at −80 mV, evokes fluorescence changes with only a fast component to the onset and recovery, consistent with the W434F mutation maintaining channels in the inactivated (fast fluorescent) state. This identifies the 424C-TMRM fast fluorescence conformation with the W434F P-type inactivated state and implies that the slow fluorescence change in response to depolarization of resting state of wild-type W434 channels is the entry into the P-type inactivated state.

ing to the resting ratio. This recovery of the slow component of F_{onset} approximately followed the recovery of the ionic current (Fig. 4 *B*). The data are consistent with channels being distributed between two states: noninactivated (slow F_{onset}) and inactivated (fast F_{onset}), with the majority of channels (85–90%) being noninactivated after a long rest at −80 mV.

424C-TMRM Fluorescence Follows W434F (P-type) Inactivation

The above observations suggest that 424C-TMRM reports on rapid gating events when the slow inactivation gate is closed, but not when that gate is open. To test this idea, and to examine the nature of the relationship between the 424C-TMRM fluorescence change and the "P-type" inactivation that has been associated with the W434F mutation (Yang et al., 1997), we examined 424C-TMRM fluorescence in W434F channels.

As shown earlier for unlabeled S424/W434F channels (Perozo et al., 1993), 424C-TMRM/W434F channels underwent the normal gating transitions associated with gating charge movement and opening but did not conduct (data not shown). We found that both the onset and recovery of the fluorescence after depolarizations of up to several seconds were fast, with no slow component (Fig. 4 *C*). F_{onset} of the W434F channel (τ = 24.3 ± 4.6; n = 7) was almost identical to the fast F_{onset} in conducting W434 channels after inactivation by a prepulse (τ = 24.7 ± 4.7; n = 9), occurring on the time scale of activation. The finding that 424C-TMRM fluorescence of W434 interconverts between the fast ΔF of W434F and the slow ΔF of resting, noninactivated channels argues that the impact on 424C-TMRM fluorescence of the W434F mutation is secondary to its influence on gating, rather than due to an influence of the side chain at 424 on the environment of the fluorophore.

The results are consistent with the idea that the slow component of the F_{onset} of 424C-TMRM monitors entry into a W434F-like inactivated state, channels must be in this state for the fluorophore at 424 to approach a neighboring protein segment and sense its rapid activation/deactivation movements. Based on the similarity between W434 channels that have been inactivated by several seconds of depolarization and W434F channels at rest, we will refer to the inactivation transition that involves a rearrangement around 424C-TMRM as P-type inactivation.

Prolonged Depolarization Stabilizes the W434F (P-type) Closed Conformation in a Manner that Resembles C-type Inactivation

Prolonged depolarization has been shown not only to inactivate channels, but to shift the voltage dependence of their gating charge movement in the hyperpolarized direction (Olcese et al., 1997), a property that has recently been used to more narrowly define "C-type" inactivation and to distinguish it from the P-type inactivation of W434F channels (Olcese et al., 1997; Yang et al., 1997). Having observed that 424C-TMRM fluorescence changed with inactivation in a manner consistent with the P-type inactivation of W434F, we next asked whether the kind of prolonged depolarization that shifts the charge–voltage relation to the left would produce a further fluorescence report.

While ionic current inactivation appeared to be complete in a few seconds, we found that depolarization for 1 min resulted in further changes. Although prolonged depolarization did not change fluorescence during the depolarizing step, it slowed the rate of both current and fluorescence recovery (Fig. 5, *A* and *B*). Similar slowing was seen in channels that retained the wild-type cysteine at position 462 and had 20-fold slower inactivation kinetics (data not shown), indicating that the slowing of both recovery from inactivation and F_{recov} of 424C-TMRM is a robust feature of the channel. In addition, depolarizations shorter than 1 min, or those of equal duration but to less depolarized voltages, had less pronounced effects (data not shown). These results suggest that after entry into a W434F-like P-type inactivated state (a rearrangement that changes the microenvironment around the NH_2-terminal end of the P-region and was therefore followed by a change in 424C-TMRM fluorescence), wild-type channels enter a second, more stable inactivated state (with a rearrangement that does not significantly change the microenvironment around 424, but which becomes rate limiting for the reverse rearrangement around 424 that reopens the slow inactivation gate). We asked whether this second inactivation rearrangement was C-type inactivation by looking at the effect of long depolarizations on F_{recov}.

Depolarizing prepulses were found to slow F_{recov} so that more negative tail potentials were necessary to obtain the same rate of F_{recov} (Fig. 5, *C* and *D*). This result could mean that recovery kinetics were generally slowed or that prolonged depolarization produces a negative shift in the voltage dependence of activation/deactivation, as found for C-type inactivation (Olcese et al., 1997). (More evidence that a negative shift in the voltage dependence of activation occurs as a separate step that follows slow inactivation gate closure is presented for the S4 labeling position, below.)

The rate of 424C-TMRM F_{recov} after prolonged depolarization was considerably faster in W434F than in W434 channels (compare Fig. 5, *A* and *E*), indicating that the W434F mutation favors entry into the P-type inactivated state from both the resting state and from the more stable, putatively C-type inactivated state.

Together, the results are consistent with the idea that inactivation proceeds in two successive steps: a first rearrangement around 424 of a W434F-like P-type inactivation that closes the external gate of the pore, and a second rearrangement that is not felt by a fluorophore at 424, that corresponds to what Olcese et al. (1997) have called C-type inactivation, which stabilizes the closed conformation of the gate, thus slowing its rate of reopening upon repolarization and of the rearrangement reported by 424C-TMRM. For simplicity, from here on we will refer to these two steps of inactivation as P- and C-type inactivation, respectively.

Ball Inactivation Accelerates Entry Into the Stabilized Inactivated Conformation

The conclusion that 424C-TMRM fluorescence directly reports closure of the slow inactivation gate implies that the accelerated F_{onset} in ball-intact channels (Fig. 2 *E*) is due to an accelerated closure of this gate. However, as mentioned above, F_{recov} in ball-intact channels was much slower than in ball-deleted channels (compare Figs. 1 *B* and 2 *E*). In fact, we found that long predepolarization produced no additional slowing of F_{recov} in ball-intact channels (Fig. 5 *G*). This suggests that, in contrast to ball-deleted channels that require tens of seconds of depolarization to enter a stabilized, C-type inactivated state, ball-intact channels C-type inactivate in only a few seconds.

S4 Movement and Slow Inactivation

The fast fluorescence behavior of P-type inactivated 424C-TMRM channels, described above, suggests that closure of the slow inactivation gate may move 424C-TMRM into the vicinity of a protein segment that is involved in activation. If this were due to a movement of 424C-TMRM into the vicinity of S4, then one would expect a reciprocal influence of the P-region on the environment of S4 to make itself felt over the time course of slow inactivation. This possibility was examined by attaching TMRM at position 359, shown earlier to lie at the outermost end of S4 (Larsson et al., 1996; Mannuzzu et al., 1996; Baker et al., 1998).

As shown earlier (Mannuzzu et al., 1996; Cha and Bezanilla, 1997), depolarization produced a rapid fluorescence decrease in 359C-TMRM/W434/C462 channels (Fig. 6 *A*). Depolarizations of many seconds produced a further slow decrease in fluorescence that correlated with slow inactivation and was followed by an F_{recov} that had fast and slow components of roughly the same amplitudes as those of the F_{onset} (Fig. 6 *A*). Depolarizations of several minutes produced a small additional fluores-

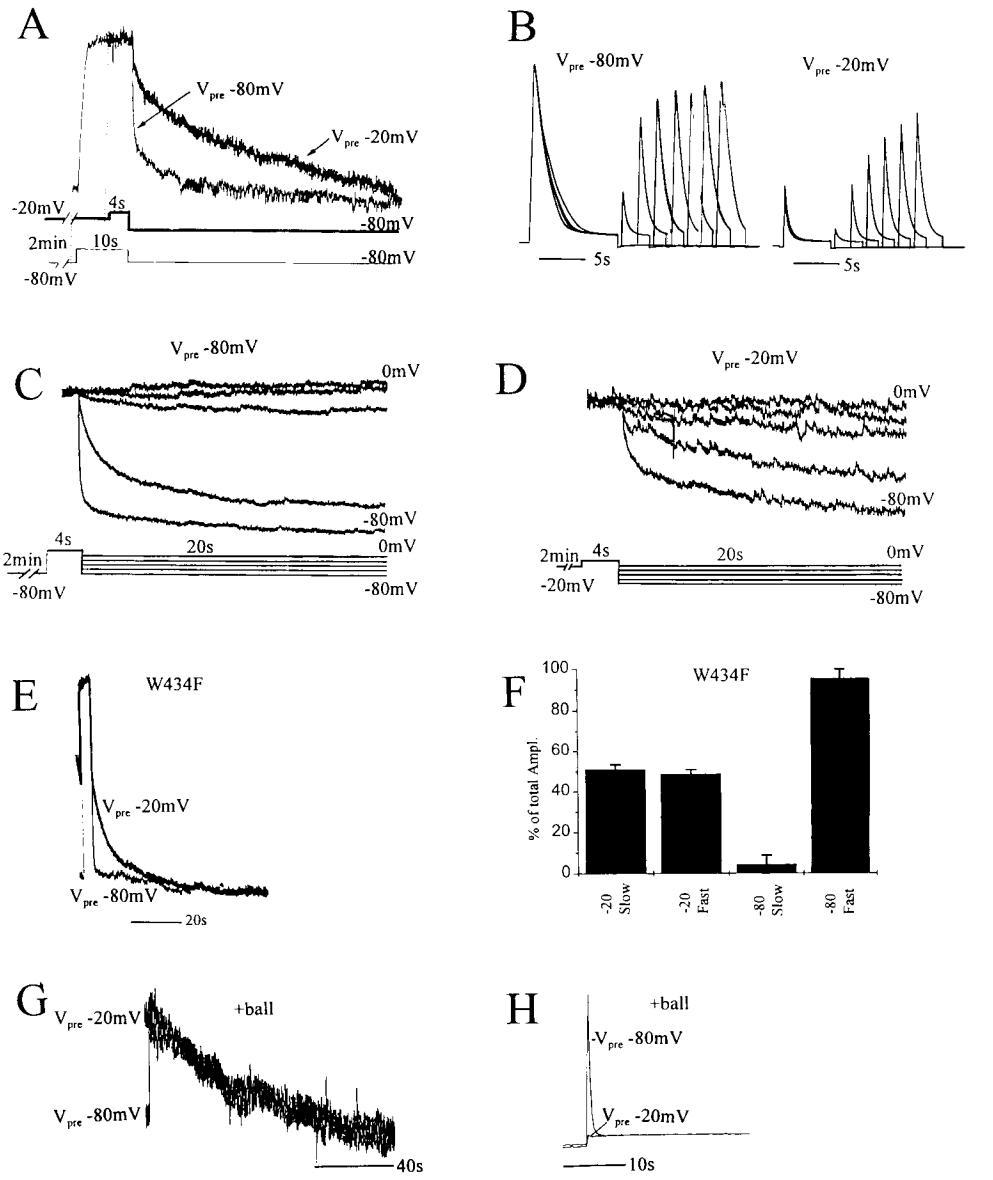

FIGURE 5. C-type inactivation slows recovery of both 424C-TMRM fluorescence and ionic current. (*A* and *B*) Recovery slowed by prolonged predepolarization. After 2 min at either −80 mV (V_{pre} −80 mV) or −20 mV (V_{pre} −20 mV), the oocyte was depolarized to +20 mV, and then returned to V_{hold} = −80 mV. Longer depolarizations were used for V_{pre} −80 mV (10 s) than for V_{pre} −20 mV (4 s) to allow the slower increase in fluorescence and slower current inactivation of V_{pre} −80 mV to reach steady state. (V_{pre} −20 mV and V_{pre} −80 mV were done in succession for each oocyte.) (*A*) F_{recov} of 424C-TMRM/W434/C462A after a step to +20 mV was slowed by a 2-min prepolarization to −20 mV (V_{pre} −20 mV) compared with control (V_{pre} −80 mV). This was a consistent finding in 10 oocytes. (*B*) Recovery of ionic current from inactivation seen in twin pulses to +20 mV requires longer intervals after a 2-min prepolarization to −20 mV (V_{pre} −20 mV) compared with control (V_{pre} −80 mV). Interval between sets of twin pulses was 2 min at V_{pre} −80 mV or V_{pre} −20 mV, with a 2.5 s return to −80 mV before the step. Responses to twin pulses at varying intervals are superimposed. (*C* and *D*) Voltage dependence of F_{recov} of 424C-TMRM/W434/C462A after a 4-s depolarization to +20 mV is altered when the step is preceded by a 2-min prepolarization to either −80 (*C*) or −20 (*D*) mV. Responses are from a single oocyte, with *D* recorded first. Successive responses to identical steps returning to different tail potentials (from −80 to 0 mV, in 20-mV increments) are superimposed. Traces are normalized to the maximum observed fluorescence change for this oocyte. (*E* and *F*) F_{recov} of 424C-TMRM/W434F/C462A in response to a step to +20 mV is mainly fast after a 2-min prepolarization to −80 mV (V_{pre} −80 mV). 2-min prepolarization to −20 mV (V_{pre} −20 mV) converts approximately half of this fast F_{recov} to a slow recovery. Two exponential fits to F_{recov} in fluorescent traces as in *E* yield component amplitudes shown in *F*. Note that F_{recov} after prepolarization to −20 mV is faster in W434F (*E*) than in W434 (*A*). (*G* and *H*) Fluorescence (*G*) and ionic current (*H*) recovery of 424C-TMRM/W434/C462A channels with the NH_2-terminal ball intact (same protocol as in *A*). (*G*) F_{recov} is as slow after prepolarization to −80 mV (V_{pre} −80 mV) as prepolarization to −20 mV (V_{pre} −20 mV). This rate is approximately equal to that of ball-deleted channels prepolarized to −20 mV (*A*), suggesting that the ball accelerates entry into the C-type inactivated state.

cence decrease. In addition, F_{recov} was altered so that the fast component represented a smaller fraction of the total, and the slow component was made substantially slower (Fig. 6 *B*). These observations suggest that three rearrangements occur in the environment of the NH_2-terminal end of S4, a fast process that takes place on the time scale of activation, a slower process that follows closure of the inactivation gate, and an even slower process that simultaneously stabilizes both S4 in its activated conformation and the inactivation gate in its closed conformation.

We asked if either of the two slow processes could be due to P-type inactivation by comparing the fluorescence behavior of wild-type W434/C462 channels to W434F/C462A channels, in which both mutations favor entry into the P-type inactivated state (Figs. 2 and

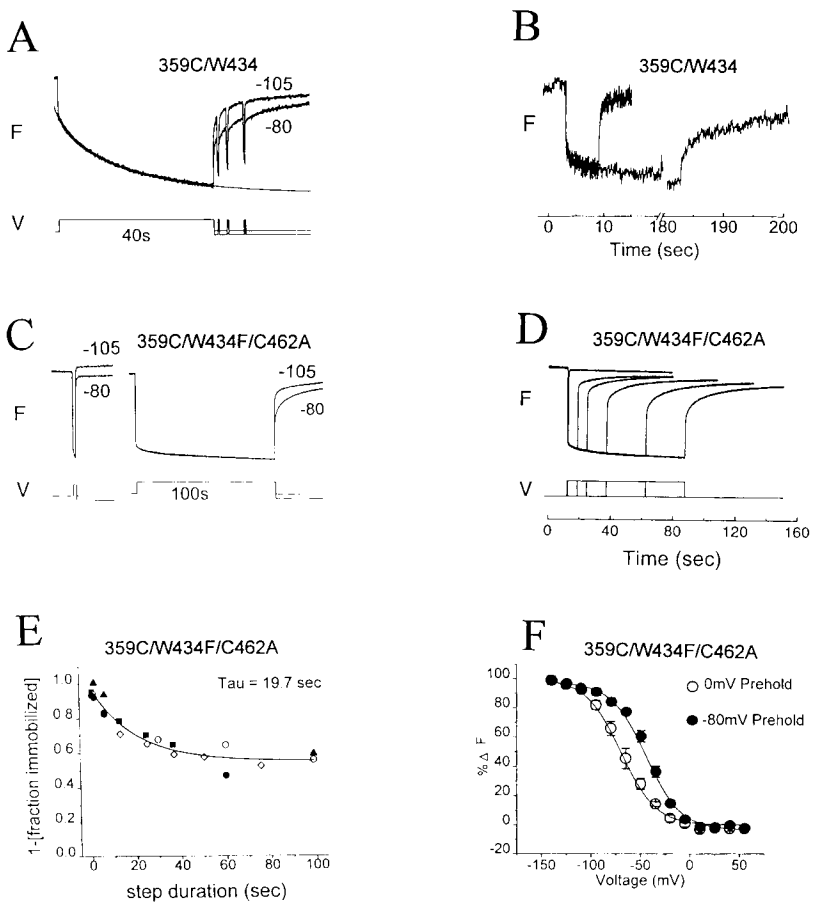

FIGURE 6. Fluorescence of 359C-TMRM reflects activation, and P- and C-type inactivation. (*A* and *B*) Fluorescence change of 359C-TMRM/C245/W434/C462 in response to depolarization (after a 2-min rest at V_{hold} = −80 mV). (*A*) The fluorescence change (step to 0 mV) has both fast and slow components. (Note that the fast component of F_{onset} is approximately equal in amplitude to the fast component of F_{recov} when $V_{tail} = V_{hold} = -80$ mV). The slow component of F_{onset} follows the inactivation of the ionic current (time course of solid line is from fit to ionic current), suggesting that a rearrangement around 359 accompanies closure of the inactivation gate. Return to a more negative (−105 mV) tail potential than V_{hold} accelerates the slow recovery. Brief depolarizations during tails of −80 mV evoke fast F_{onset} similar to that of the first depolarization. (*B*) Long (3-min) depolarization (from V_{hold} = −80 mV to V_{step} = +20 mV) reduces the amplitude of the fast component of F_{recov} and slows the slow component (compare with *A*). (*C* and *D*) Fluorescence change of 359C-TMRM/C245/W434F/C462A in response to depolarization (to 0 mV after a 2-min rest at V_{hold} = −80 mV). (*C*) Short depolarization yields mainly fast components of F_{onset} and F_{recov}. Long depolarization evokes a small slow component of F_{onset} and alters F_{recov} by reducing the amplitude of the fast component and further slowing the slow component. Responses are superimposed for tail potentials of −80 and −105 mV. (*D*) The degree of reduction in amplitude of the fast component of F_{recov} increases with increasing duration of depolarization, roughly in parallel to the slow decrease of fluorescence during the step. (*E*) Relation of reduction in amplitude (immobilization) of the fast component of F_{recov} to step duration, measured from traces such as *D*. Data from five oocytes (each oocyte = one symbol) combined and fit to a single exponential (*solid line*). (*F*) Long (2-min) predepolarization (to 0 mV) shifts, in the negative direction, the voltage dependence of the fast fluorescence–voltage relation. Fluorescence was measured at the end of 200-ms steps to indicated potentials that are primarily from the fast component of fluorescence change. Steps were given at 4-s intervals to permit recovery from small amounts of inactivation induced by positive steps from V_{hold} = −80 mV, or to permit reentry into the inactivated state after small amounts of recovery during negative steps from V_{hold} = 0 mV. Data from five oocytes. Note that return to a more negative (−105 mV) tail potential than V_{hold} (−80 mV) makes the fast component larger in the recovery for both W434 (*A*) and W434F/C462A (*C*) because a larger fraction of S4s enter their resting conformation.

4). 359C-TMRM/W434F/C462A channels had both fast and slow components of fluorescence change (Fig. 6 *C*), but the fractional amplitude of the slow component was ~2.5-fold greater in W434/C462 than in W434F/C462A (0.42 ± 0.6, n = 4 and 0.17 ± 0.1, n = 6, respectively; compare Fig. 6, *A* and *C*). This finding implies that P-type inactivation is responsible for part, but not all, of the slow component of F_{onset} of 359C-TMRM.

Depolarizations of 359C-TMRM/W434F channels that were long enough to evoke a measurable slow component of F_{onset}, following the fast component, recovered in fast and slow components. The size of the fast component of F_{recov} during the tail became smaller with increasing step duration, roughly in parallel to the slow component of F_{onset} (Fig. 6, *D* and *E*). This reduction in fast F_{recov} amplitude was almost completely overcome if the tail potential was made 25 mV more negative than the holding potential (Fig. 6 *C*). The effect of tail potential suggests that the prolonged depolarization resulted in a stabilization of the activated state, as shown earlier to occur with C-type inactivation (Olcese et al., 1997).

This hypothesis was addressed by comparing the F-V relation of resting and inactivated 359C-TMRM/W434F/C462A channels by applying short steps after a prolonged (2-min) conditioning step to either −80 or 0 mV, respectively. As shown earlier for charge movement in W434F channels (Olcese et al., 1997), a sustained predepolarization to 0 mV shifted the voltage dependence of S4 movement by ~−25 mV (Fig. 6 *F*), showing that the effect on the charge movement can be accounted for by a stabilization of the S4 in its activated (extruded) transmembrane position. Such stabilization could explain, at least in part, how C-type inactivation slows the reopening of the inactivation gate.

Taken together, the results are consistent with three successive S4 rearrangements in response to depolarization: fast transmembrane activation movement, followed by a P-type inactivation closure, followed in turn by C-type inactivation, which stabilizes the closed conformation of the inactivation gate. The W434F/C462A mutations appear to limit the gating range to the subset in which S4 can move across the membrane, but the inactivation gate remains closed, transiting between its P- and C-type inactivated conformations.

DISCUSSION

Structural Rearrangements Underlying Slow Inactivation

Our observations are consistent with the idea that slow inactivation of the *Shaker* K^+ channel proceeds in two sequential steps: a first step that closes a gate at the external mouth of the pore and a second step that stabilizes the gate in its closed conformation. We distinguish between these two states of the channel in which the external gate is closed as the P- and C-type inactivated state, respectively, based on criteria discussed below.

This interpretation is based on observed changes in TMRM fluorescence at two attachment sites that correlate with slow inactivation of the ionic current. One of the TMRM attachment sites, position 424, is at the NH_2-terminal end of the P-region and lies near the perimeter of the outer mouth of the pore, as shown by toxin footprint experiments (Gross and MacKinnon, 1996). This position is located in the middle of the "turret," a segment with an extended secondary structure, at the NH_2-terminal side of the helical and selectivity segments of the P-region seen in the crystal structure for the KcsA channel (Doyle et al., 1998), a bacterial channel with structural homology to *Shaker* (Mackinnon et al., 1998). The other site, position 359, lies at the NH_2-terminal end of S4 and represents one of the most external positions in S4 to be buried in the transmembrane protein when S4 is retracted into the cell in the resting state (Larsson et al., 1996; Yusaf et al., 1996; Baker et al., 1998). Position 359 labeled with TMRM had been studied previously (Mannuzzu et al., 1996; Cha and Bezanilla, 1997), but its role in inactivation was not studied because only short depolarizations were used in nonconducting channels. While fluorescence measurements for position 424 have not been previously described, Cha and Bezanilla (1997) used Oregon green at 425 and found, as we did for 424-TMRM, that it has an F-V that is steeper than the G-V, though they did not describe the kinetics of the fluorescence change.

The results indicate that a change in the protein microenvironment around positions 359 and 424 accompanies closure and opening of the slow inactivation gate. This could mean that the rearrangements at the COOH-terminal end of the P-region, which were previously correlated with slow inactivation (Yellen et al., 1994; Liu et al., 1996), occur in the immediate environment of the NH_2 terminal of the P-region and of S4. Alternatively, either the NH_2 terminal of the P-region or S4 (or both) may undergo a coordinated movement along with the COOH-terminal end of the P-region to open and close the slow inactivation gate.

The finding that 424C-TMRM reports on activation/deactivation when the slow inactivation gate is closed, but not when it is open, suggests that the structural relation between the NH_2 terminal of the P-region and S4 changes with this gating. A possible explanation for the present observations, and for those of Yellen et al. (1994) and Liu et al. (1996), is that the entire P-region undergoes a coordinate rearrangement to open and close the inactivation gate, and that this changes the environment around the NH_2 termini of the P-region and of S4 by increasing P-S4 proximity.

A clue as to the nature of this closing rearrangement comes from the finding of possible van der Waals interactions and hydrogen bonding between a signature sequence tyrosine, whose backbone interacts with permeant ions, and the tryptophan in KscA that is analogous to W434 (Doyle et al., 1998). Removing the terminal ring of the tryptophan by mutation to phenylalanine, as in the mutation W434F, which locks the inactivation gate in the closed conformation, would be expected to break such interaction. This suggests that closure of the inactivation gate in wild-type channels involves breaking of this tryptophan–tyrosine interaction and that, based on our fluorescence measurements, this leads to a rearrangement of the turret that increases its proximity to S4. For the turret to respond to a break in interaction with a residue in the nearby P-region helix, a unified motion of turret and helix may have to occur that swings mid-turret to face S4, and possibly changes the tilt of the helix. In any case, the rearrangement may collapse the binding site formed by the signature tyrosine, which is the outer of two permeant ion binding sites in KscA (Doyle et al., 1998). Such a model is compatible with the finding that closure of the slow inactivation gate pinches off access between the external solution and a deep permeant ion binding site near *Shaker* residue 441 (Harris et al., 1998), analogous to a conserved residue near the internal permeant binding site of KscA (Doyle et al., 1998).

P- and C-type Inactivation

Since K^+ channels were first cloned, their slow inactivation has been referred to by the single rubric "C-type inactivation." Recently, however, it has been suggested that there exist at least two distinct processes of inactivation. One of these is highly favored by the W434F mutation and permits channels to undergo normal voltage-dependent gating charge and opening rear-

rangements (Perozo et al., 1993; Yang et al., 1997). The second alters the voltage dependence of charge movement and proceeds from both resting closed states in wild-type channels and from the P-inactivated state in W434F channels (Olcese et al., 1997).

Our findings are consistent with a simple model in which slow inactivation is mediated by a single molecular gate, which can be closed in two states with differing stabilities. We attribute the difference in stability between these two closed states of the gate to differences in the conformation around the voltage sensor. In the versions of *Shaker* H4 and under the range of ionic conditions explored here, entry into the less stable, P-type inactivated closed state occurs quickly under sustained depolarization, and this is followed by a slower entry into the more stable closed C-type state. At least part of this stabilization of the closed conformation of the gate is due to a C-type inactivation rearrangement of or around S4 that stabilizes S4 in its extruded conformation (so that stronger electric fields are needed to return it to its resting conformation), thus slowing S4's deactivation transmembrane movement. This explains the effect of C-type inactivation on gating charge movement, observed previously (Olcese et al., 1997), and provides insight into the complex voltage and time dependence of slow inactivation.

Three Tiers of Gating

Our results suggest a three-tiered scheme (Fig. 7), in which prolonged duration at negative voltage accumulates channels in a resting state with a closed internal activation gate and open external slow inactivation gate (*top left*). Millisecond-long depolarizations, followed by repolarization, activate and then deactivate primarily in the top tier. Second-long depolarizations provide enough time for channels to accumulate in the second tier (P-type inactivation closure of external gate) from activated states; this rearrangement is proposed to increase the proximity of the NH_2 termini of S4 and the P-region.

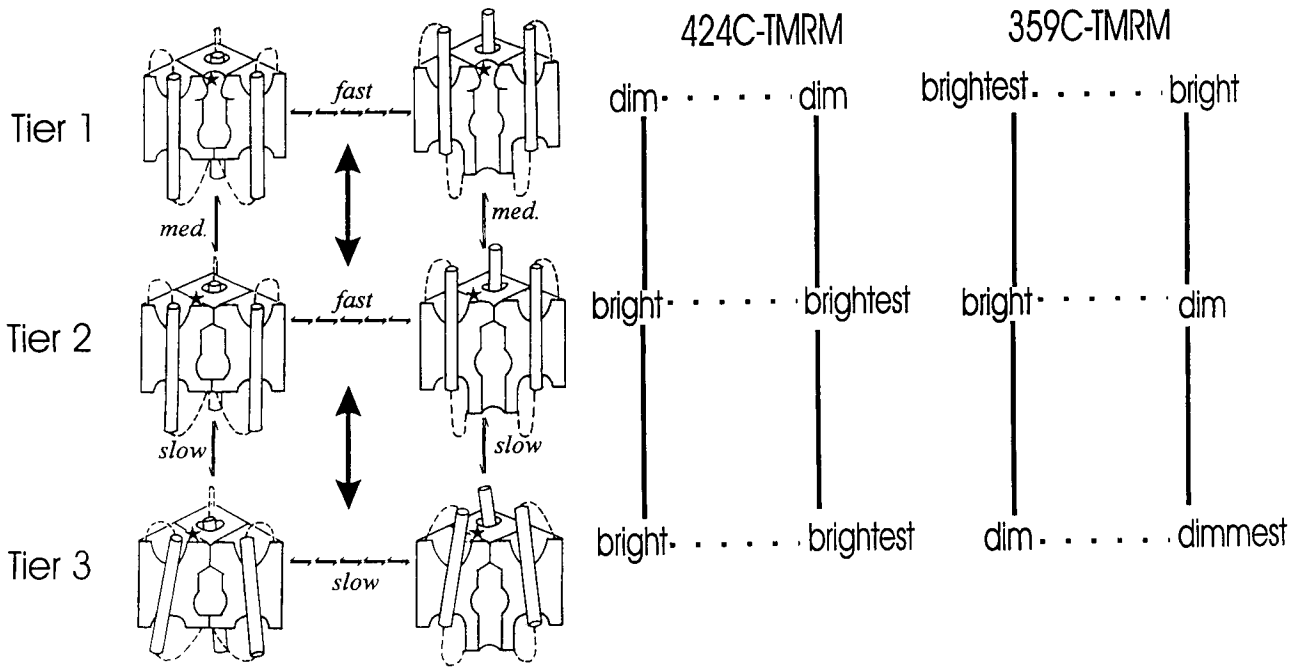

FIGURE 7. Gating model of slow inactivation. (*left*) The scheme depicts proposed conformations of S4, the internal activation gate, and the external inactivation gate in channels with the external inactivation gate open (*Tier 1*), or closed in the P-type (*Tier 2*) or C-type (*Tier 3*) inactivated conformations (*attachment site 424 in the NH_2-terminal end of the P-region). The model is based on observations of the relative brightness of TMRM at attachment sites 424 in the P-region (*middle*) and 359 in S4 (*right*). P-type inactivation (*Tier 1* → *2*) and its recovery (*Tier 2* → *1*) are, respectively, the rearrangements that close and open the external gate. C-type inactivation (*Tier 2* → *3*) and its recovery (*Tier 3* → *2*) are, respectively, the rearrangements that stabilize and destabilize the closed conformation of the external gate. Depolarization drives channels to the right in all tiers so that they extrude their S4s, open their internal activation gates, and are favored to enter the next tier down. Hyperpolarization drives channels to the left, closes the activation gate, retracts the S4s, and drives channels to higher tiers. Gating in Tier 1 does not alter the fluorescence of 424C-TMRM (the small fast component of F_{onset} after rest at −80 mV is taken to represent a minority of channels in Tier 2 at the resting potential), but does produce a fluorescence change in 359C-TMRM. In Tiers 2 and 3, the external slow inactivation gate is closed and both 424C-TMRM and 359C-TMRM follow transmembrane movement of S4. Tier 3 has slower deactivation kinetics than Tier 2, due to stabilization of the S4 extruded conformation. This stabilization may involve a rearrangement around S4 (possibly in the P-region, not depicted), or, as depicted, a tilt in S4. The W434F mutation stabilizes the P-type inactivated closed conformation, concentrating channels in Tier 2 while still permitting excursions to Tier 3.

Longer depolarizations permit further entry into the activated side of the third tier (C-type inactivation stabilizes the closed conformation of the external gate); this involves some further rearrangement around S4, which is depicted as a tilt of S4 in Fig. 7.

In Fig. 7, deactivation is slower in Tier 3 than in Tiers 1 and 2 because of the shift in the voltage dependence of activation/deactivation that accompanies C-type inactivation. We can account for that shift by the observed increase in the relative stability of S4 in its activated transmembrane position. The absence of intrinsic voltage dependence for the rate of onset of slow inactivation shown earlier (Hoshi et al., 1991; Olcese et al., 1997), and for that of P-type inactivation, shown here, is consistent with the idea that the P- and C-type inactivation movements of S4 are parallel to the membrane electric field. The choice of single step transition between the tiers is motivated by earlier evidence that slow inactivation is cooperative (Ogielska et al., 1995; Panyi et al., 1995). Under an allosteric scheme such as that proposed by Olcese et al. (1997), this cooperativity can account for our observation that the steady state voltage dependence of P-type inactivation is steeper than that of channel opening. The simplest explanation of our observations is presented here, although we cannot rule out more complex models involving multiple slow inactivation gates.

Gating Rearrangements of Inactivated Channels

Starkus et al. (1997) demonstrated the ability of the channel to undergo deactivation in the inactivated state by altering external solutions and watching Na^+ flux. Here, we show activation and deactivation in both P- and C-type inactivated channels under physiological ionic conditions. Since voltage clamp fluorometry reports on protein movements even when these do not produce a measurable electrical change, it enabled us to obtain a continuous measure of the opening and closing of one gate in a channel in which another gate is closed; that is, in the absence of a change in ionic or gating current. Such measurements suggest that the P- and C-type inactivated states have the same conformation in the NH_2-terminal end of the P-region, but that C-type inactivation produces an additional rearrangement about the NH_2-terminal end of S4. Our measurements further show that the acceleration of slow inactivation in N-type inactivated (NH_2-terminal ball blocked) channels (Baukrowitz and Yellen, 1995) appears to involve acceleration of both the P- and C-type inactivation processes.

Thus, N-type inactivation can trap channels in the activated state by two means: directly by preventing deactivation for as long as the NH_2-terminal ball occupies the internal mouth of the channel, as shown earlier (Bezanilla et al., 1991), and indirectly by accelerating entry into the C-type inactivated conformation, which stabilizes the activated conformation of S4, as shown here. The stabilization of the extruded conformation of S4 by C-type inactivation helps explain how the onset of inactivation can be time dependent but intrinsically voltage independent, while its recovery is voltage dependent. Finally, the finding that channels maximally P-type inactivate at voltages that are not sufficient to maximally open them indicates that it is the transmembrane disposition of S4, rather than the state of the activation gate, that determines the conformation of the external inactivation gate (see Baukrowitz and Yellen, 1995).

Conclusion

Our results implicate both the P-region and S4 voltage sensor in the conformational changes that close the external inactivation gate of the *Shaker* K^+ channel, and are consistent with the idea that gate closure alters the interaction between these domains. We find that inactivation via this external gate is governed by the transmembrane topology of S4 and that a rearrangement about S4 consolidates inactivation by making it more difficult for S4 to be retracted back into its resting topology. These findings provide a concrete picture of how a gate, whose movements are intrinsically voltage independent, is coupled to the voltage sensor and, therefore, controlled by the electric field.

We thank all members of the lab, J. Ngai and H. Lecar for helpful discussion, O. Baker for advice on data analysis, L. Mannuzzu, K. Glauner, and O. Baker for their groundwork on the 359C- and 424C-labeled channels, L. Llewellyn for help in making the linked tetramers, and C. Dean for the scheme in Fig. 7.

The work was funded by National Institutes of Health grant NS35549-01, American Heart Foundation, California Affiliate grant 96-248A, and an award from the Lucille P. Markey Fund for Innovation.

Original version received 12 May 1998 and accepted version received 3 August 1998.

REFERENCES

Baker, O.S., H.P. Larsson, L.M. Mannuzzu, and E.Y. Isacoff. 1998. Three transmembrane conformations and sequence-dependent displacement of the S4 domain in *Shaker* K^+ channel gating. *Neuron.* 20:1283–1294.

Baukrowitz, T., and G. Yellen. 1995. Modulation of K^+ current by frequency and external $[K^+]$: a tale of two inactivation mecha-

nisms. *Neuron.* 15:951–960.

Baukrowitz, T., and G. Yellen. 1996. Use-dependent blockers and exit rate of the last ion from the multi-ion pore of a K^+ channel. *Science.* 271:653–656.

Bezanilla, F., E. Perozo, D. Papazian, and E. Stefani. 1991. Molecular basis of gating charge immobilization in *Shaker* potassium channels. *Science.* 254:679–683.

Boland, L., M. Jurman, and G. Yellen. 1994. Cysteines in the *Shaker* K channel are not essential for channel activity or zinc modulation. *Biophys. J.* 66:694–699.

Cha, A., and F. Bezanilla. 1997. Characterizing voltage-dependent conformational changes in the *Shaker* K channel with fluorescence. *Neuron.* 19:1127–1140.

De Biasi, M., H.A. Hartman, J.A. Drewe, M. Tagialatela, A.M. Brown, and G.E. Kirsh. 1993. Inactivation determined by a single site in K^+ pores. *Pflügers Arch. Eur J. Physiol.* 422:354–363.

Doyle, D.A., J.M. Cabral, R.A. Pfuetzner, A. Kuo, J.M. Gulbis, S.L. Cohen, B.T. Chait, and R. Mackinnon. 1998. The structure of the potassium channel: molecular basis of K^+ conduction and selectivity. *Science.* 280:69–77.

Gross, A., and R. MacKinnon. 1996. Agitoxin footprinting the *Shaker* potassium channel pore. *Neuron.* 16:399–406.

Harris, R.E., H.P. Larsson, and E.Y. Isacoff. 1997. A permeant ion binding site located between two gates of the *Shaker* K^+ channel. *Biophys. J.* 74:1808–1820.

Heginbotham, L., Z. Lu, T. Abramson, and R. MacKinnon. 1994. Mutations in the K channel signature sequence. *Biophys. J.* 66: 1061–1071.

Hoshi, T., W.N. Zagotta, and R.W. Aldrich. 1990. Biophysical and molecular mechanisms of *Shaker* potassium channel inactivation. *Science.* 250:533–538.

Hoshi, T., W. Zagotta, and R. Aldrich. 1991. Two types of inactivation in *Shaker* K channels: effect of alterations in the carboxyterminal region. *Neuron.* 7:547–556.

Isacoff, E., Y. Jan, and L. Jan. 1990. Evidence for the formation of heteromultimeric potassium channels in *Xenopus* oocytes. *Nature.* 345:530–534.

Isacoff, E., Y. Jan, and L. Jan. 1991. Putative receptor for the cytoplasmic inactivation gate in the *Shaker* K channel. *Nature.* 353:86–90.

Iverson, L.E., and B. Rudy. 1990. The role of the divergent amino and carboxyl domains on the inactivation properties of potassium channels derived from the *Shaker* gene of Drosophila. *J. Neurosci.* 10:2903–2916.

Kunkel, T.A. 1985. Rapid and efficient site-specific mutagenesis without phenotypic selection. *Proc. Natl. Acad. Sci. USA.* 82:488–492.

Kurz, L., R.D. Zuhlke, H. Zhang, and R. Joho. 1995. Side-chain accessibilities in the pore of a K channel probed by sulfhydryl-specific reagents after cysteine-scanning mutagenesis. *Biophys. J.* 68: 900–905.

Larsson, H.P., O.S. Baker, D.S. Dhillon, and E.Y. Isacoff. 1996. Transmembrane movement of the *Shaker* K^+ channel S4. *Neuron.* 16:387–397.

Levy, D., and C. Deutsch. 1996. Recovery from c-type inactivation is modulated by extracellular potassium. *Biophys. J.* 70:798–805.

Lopez-Barneo, J., T. Hoshi, S. Heinemann, and R. Aldrich. 1993. Effects of external cations and mutations in the pore region on c-type inactivation of *Shaker* potassium channels. *Receptors Channels.* 1:61–71.

Liu, Y., M. Jurman, and G. Yellen. 1996. Dynamic rearrangement of the outer mouth of a K channel during gating. *Neuron.* 16:859–867.

Lu, Q., and C. Miller. 1995. Silver as a probe of pore-forming residues in a potassium channel. *Nature.* 268:304–307.

MacKinnon, R., S.L. Cohen, A. Kuo, A. Lee, and B.T. Chait. 1998. Structural conservation in prokaryotic and eukaryotic potassium channels. *Science.* 280:106–109.

Mannuzzu, L., M. Moronne, and E.Y. Isacoff. 1996. Direct physical measure of conformational rearrangement underlying potassium channel gating. *Science.* 271:213–216.

Marom, S., and I. Levitan. 1994. State-dependent inactivation of the Kv3 potassium channel. *Biophys. J.* 67:579–589.

Naranjo, D., and C. Miller. 1996. A strongly interacting pair of residues on the contact surface of charybdotoxin and a *Shaker* K channel. *Neuron.* 16:123–130.

Ogielska, E.M., W. Zagotta, T. Hoshi, S. Heinemann, J. Haab, and R. Aldrich. 1995. Cooperative subunit interactions in C-type inactivation of K channels. *Biophys. J.* 69:2449–2457.

Olcese, R., R. Latorre, L. Toro, F. Bezanilla, and E. Stefani. 1997. Correlation between charge movement and ionic current during slow inactivation in *Shaker* K^+ channels. *J. Gen. Physiol.* 110:579–589.

Panyi, G., Z. Sheng, L. Tu, and C. Deutsch. 1995. C-type inactivation of a voltage-gated channel occurs by a cooperative mechanism. *Biophys. J.* 69:896–903.

Pascual, J., C. Shieh, G. Kirsch, and A. Brown. 1995. K pore structure revealed by reporter cysteines at inner and outer surfaces. *Neuron.* 14:1055–1063.

Perozo, E., R. MacKinnon, F. Bezanilla, and E. Stefani. 1993. Gating currents from a nonconducting mutant reveal open–closed conformations in *Shaker* K^+ channels. *Neuron.* 11:353–358.

Starkus, J.G., L. Kuschel, M. Rayner, and S. Heinemann. 1997. Ion conduction through c-type inactivated *Shaker* channels. *J. Gen. Physiol.* 110:539–550.

Timpe, L., Y. Jan, and L. Jan. 1988. Four cDNA clones from the *Shaker* locus of Drosophila induce kinetically distinct A-type potassium currents in *Xenopus* oocytes. *Neuron.* 1:659–667.

Yang, Y., Y. Yan, and F. Sigworth. 1997. How does the W434F mutation block current in the *Shaker* potassium channels? *J. Gen. Physiol.* 109:779–789.

Yellen, G., D. Sodickson, T. Chen, and E. Jurman. 1994. An engineered cysteine in the external mouth of a K channel allows inactivation to be modulated by metal binding. *Biophys. J.* 66:1068–1075.

Yool, A.J., and T.L. Schwarz. 1991. Alterations of ionic selectivity of a K channel by mutation of the H5 region. *Nature.* 349:700–704.

Yusaf, S.P., D. Wray, and A. Sivaprasadarao. 1996. Measurement of the movement of the S4 segment during the activation of a voltage-gated potassium channel. *Pflügers Arch.* 433:91–97.

Zagotta, W.N., T. Hoshi, and W. Aldrich. 1990. Restoration of inactivation in mutants of *Shaker* potassium channels by a peptide derived from ShB. *Science.* 250:568–571.